Supporting Information

A ratiometric, fluorescent BODIPY-based probe for transition and heavy metal ions

Wenwu Qin,[#,*] Wei Dou,[#] Volker Leen,[†] Wim Dehaen,[†] Mark Van der Auweraer[†] and Noël Boens[†,*]

[#] *Key Laboratory of Nonferrous Metal Chemistry and Resources Utilization of Gansu Province and State Key Laboratory of Applied Organic Chemistry, College of Chemistry and Chemical Engineering, Lanzhou University, Lanzhou 730000, China*

[†] *Department of Chemistry, KU Leuven (Katholieke Universiteit Leuven), Celestijnenlaan 200f, 3001 Leuven, Belgium*

Contents

[*] Corresponding authors: E-mail: qinww@lzu.edu.cn (W. Qin) and Noel.Boens@chem.kuleuven.be (N. Boens)

Experimental

Materials

All solvents for the spectroscopic measurements were of spectroscopic grade and were used without further purification. Metal perchlorates of the highest purity available were purchased from Beijing J & K Chemical Technology Co (Beijing, China) and were dried in a vacuum oven before use. The chemicals for the synthesis were of reagent grade quality, procured from commercial sources, and used as received.

Steady-state UV–vis absorption and fluorescence spectroscopy

Dilute solutions of **1** in different solvents were prepared by dissolving the dry, powered dye in the appropriate solvent so that the absorbance at the maximum of the main absorption peak was ≤ 0.1 using 1-cm optical path length (corresponding to a dye concentration in the μM range). UV–vis absorption spectra were recorded on a Varian UV-Cary100 spectrophotometer, and for the corrected steady-state excitation and emission spectra, a Hitachi F-4500 spectrofluorometer or an Edinburgh Instruments FLS920 was employed. Freshly prepared samples in 1-cm quartz cells were used to perform all UV–vis absorption and emission measurements. For the determination of the fluorescence quantum yields Φ of **1**, only dilute solutions with an absorbance below 0.1 at the excitation wavelength (λ_{ex} = 530 nm, except for DMF, CH_3CN and DMSO with λ_{ex} = 510 nm) were used. Cresyl violet in methanol (Φ_r = 0.55) was used as fluorescence reference.[1] The Φ values reported in Table 1 are the averages of three fully independent measurements. The standard uncertainties on the Φ values were 0.01–0.02. In all cases, correction for the solvent refractive index was applied. All spectra were recorded at 20 °C using nondegassed samples.

Determination of K_d through *direct* fluorometric titration

The ground-state dissociation constants K_d of the complexes between **1** and various cations were determined in CH_3CN solution at 20 °C by *direct* fluorometric titration as a function of the cation concentration [X] using the fluorescence excitation or emission spectra. Nonlinear fitting of eqn 3 to the steady-state fluorescence data F recorded as a function of [X] yields values of K_d, F_{min}, F_{max} and n.[2]

Determination of K_d through *ratiometric* fluorometric titration

If spectral shifts are observed in the excitation and/or emission spectra upon binding of the cation X by the probe, then *ratiometric* fluorometric titrations as a function of the cation concentration [X] – using ratios of the fluorescence excitation or emission spectral data – can be used to determine K_d and n of the probe–cation complex. This is the case for **1** and various cations. Nonlinear fitting of eqn 4 to the steady-state fluorescence ratios R recorded as a function of [X] yields values of $K_d\xi$, R_{min}, R_{max} and n.[2]

Solvent dependence of absorption and fluorescence emission maxima

The solvent effect on the physicochemical observable y is described by the multilinear expression 1:

$$y = y_0 + a_{SA}\,SA + b_{SB}\,SB + c_{SP}\,SP + d_{SdP}\,SdP \quad (1)$$

where y_0 denotes the physicochemical property of interest in the gas phase; a_{SA}, b_{SB}, c_{SP} and d_{SdP} are adjustable coefficients that reflect the dependency of the physicochemical property y in a given solvent on the {SA, SB, SP, SdP} solvent parameters. SA, SB, SP and SdP are four mutually independent, empirical solvent scales – introduced by Catalan[3] – that characterize respectively the solvent acidity, basicity, polarizability and dipolarity. The physicochemical characteristics y analyzed are the absorption maxima $\bar{\nu}_{abs}$ [= $1/\lambda_{abs}(max)$] and the fluorescence emission maxima $\bar{\nu}_{em}$ [= $1/\lambda_{em}(max)$], both expressed in cm^{-1}. The {SA, SB, SP, SdP} parameters for an extensive list of solvents can be found in ref. 3.

The advantage of the generalized (i.e., Catalán) treatment of the solvent effect over all the other approaches is that it allows one to disentangle the relative contributions of dipolarity, polarizability, acidity and basicity of the medium. Hence, it is instructive to determine by the Catalán methodology which solvent properties contribute primarily to the observed solvatochromic shifts of $\bar{\nu}_{abs}$ and $\bar{\nu}_{em}$.

The fit of $\bar{\nu}_{abs}$ of **1** according to eqn 1 with {SA, SB, SP, SdP} as independent variables yields a large d_{SdP} estimate with high precision (i.e., comparatively small standard error) in relation to {a_{SA}, b_{SB}, c_{SP}} with relatively high standard errors (Table S1). This is indicative that the change of $\bar{\nu}_{abs}$ reflects predominantly a change in dipolarity of the environment of the dye. The large positive d_{SdP}-value is in agreement with the fact that more (di)polar solvents (increasing SdP) produce a hypsochromic shift of $\lambda_{abs}(max)$ (i.e., larger $\bar{\nu}_{abs}$). This suggests a decreased dipole moment of **1** in S_1 compared to S_0. If SdP was left out as independent variable in the analyses of $\bar{\nu}_{abs}$ of **1** according to eqn 1 (that is, with {SA, SB, SP}), a low r-value (0.172) was found, implying the importance of this solvent parameter. Conversely, the three analyses of $\bar{\nu}_{abs}$ according to eqn 1, in which the common independent variable is SdP (i.e., with {SA, SB, SdP}, {SB, SP, SdP} and {SA, SP, SdP} as independent variables), all gave high-quality fits (with r = 0.935, 0.883 and 0.939, respectively). Further corroboration for SdP as major factor comes from the six analyses with two solvent scales as independent variables: the three analyses with SdP (i.e., with {SA, SdP}, {SB, SdP} and {SP, SdP}) all gave high r-values (> 0.862), whereas the three other analyses (without SdP) yielded unacceptable fits (r < 0.171). The crucial role of solvent dipolarity was finally confirmed by the high-quality linear relationship (r = 0.860) between $y = \bar{\nu}_{abs}$ and SdP and the inadequate linear fits of $y = \bar{\nu}_{abs}$ as a function of SA, SB and SP, respectively (r = 0.137, 0.017 and 0.065, respectively). Additional evidence that solvent polarizability does not influence the position of $\bar{\nu}_{abs}$ can be inferred from the unacceptable fit of $y = \bar{\nu}_{abs}$ vs. $f(n) = (n^2 - 1)/(2n^2 + 1)$ (r = 0.271).

The Catalán {SA, SB, SP, SdP} solvent scales (eqn 1) also describe adequately the solvatochromic shifts of $\bar{\nu}_{em}$ (r = 0.827, Table S1). To find out which solvent properties predominantly account for the shifts of $\bar{\nu}_{em}$, we performed some additional regression analyses according to eqn 1 in which systematically one, two and three solvent scales were omitted. These analogous analyses of $\bar{\nu}_{em}$ of **1** indicated that dipolarity is the main factor determining the position of $\bar{\nu}_{em}$. For example, the analyses in which one solvent scale was omitted clearly identify solvent dipolarity as the most critical one for $\bar{\nu}_{em}$. Indeed, the three analyses of $\bar{\nu}_{em}$ according to eqn 1, in which SdP is the common independent variable, all gave fits with r between 0.803 and 0.825. In contrast, the analysis of $\bar{\nu}_{em}$ according to eqn 1, in which solvent dipolarity was left out, produced a much lower low r-value (0.218). Hence, as found for $\bar{\nu}_{abs}$, solvent dipolarity is the most important solvent property determining the position of $\bar{\nu}_{em}$ and this is confirmed by the linear regression of $y = \bar{\nu}_{em}$ vs. SdP (r = 0.790). Extra corroboration that solvent polarizability does not determine the position of $\bar{\nu}_{em}$ can be inferred from the unacceptable fit of $y = \bar{\nu}_{em}$ vs. $f(n) = (n^2 - 1)/(2n^2 + 1)$ (r = 0.415).

Table S1. Estimated coefficients (y_0, a_{SA}, b_{SB}, c_{SP}, d_{SdP}; eqn 1), their standard errors and correlation coefficients (r) for the multilinear regression analyses of $\bar{\nu}_{abs}$ and $\bar{\nu}_{em}$ of **1** for the solvents listed in Table 1 as a function of the Catalán solvent scales. The estimates are expressed in cm^{-1}.

	y_0	a_{SA}	b_{SB}	c_{SP}	d_{SdP}	r
$\bar{\nu}_{abs}$	$(18.2 \pm 0.5) \times 10^3$	-841 ± 249	-54 ± 170	-625 ± 649	$(1.3 \pm 0.1) \times 10^3$	0.939
$\bar{\nu}_{abs}$	$(17.8 \pm 0.6) \times 10^3$		-305 ± 201	71 ± 812	$(1.2 \pm 0.2) \times 10^3$	0.883
$\bar{\nu}_{abs}$	$(18.1 \pm 0.4) \times 10^3$	-876 ± 217		-610 ± 626	$(1.3 \pm 0.1) \times 10^3$	0.939
$\bar{\nu}_{abs}$	$(17.7 \pm 0.1) \times 10^3$	-765 ± 236	-42 ± 169		$(1.3 \pm 0.1) \times 10^3$	0.935
$\bar{\nu}_{abs}$	$(18.3 \pm 0.1) \times 10^3$	-401 ± 677	183 ± 464	137 ± 1780		0.172
$\bar{\nu}_{em}$	$(17.2 \pm 0.3) \times 10^3$	-178 ± 142	31 ± 97	-474 ± 371	392 ± 77	0.827
$\bar{\nu}_{em}$	$(17.1 \pm 0.3) \times 10^3$		-22 ± 89	-327 ± 359	374 ± 77	0.804
$\bar{\nu}_{em}$	$(17.2 \pm 0.3) \times 10^3$	-158 ± 124		-483 ± 358	395 ± 73	0.825
$\bar{\nu}_{em}$	$(168.5 \pm 0.6) \times 10^2$	-120 ± 138	41 ± 99		380 ± 78	0.803
$\bar{\nu}_{em}$	$(17.2 \pm 0.4) \times 10^3$	-45 ± 234	103 ± 161	-244 ± 616		0.218

Binding of transition metal and heavy metal ions by 1

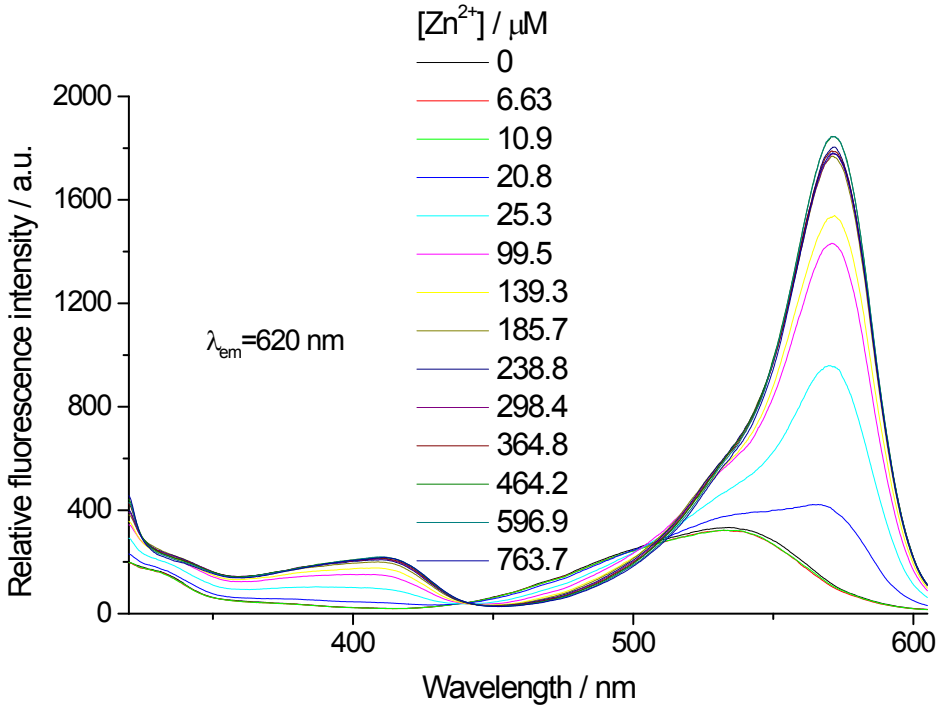

Figure S1. Fluorescence excitation spectra of compound **1** in acetonitrile solution as a function of $[Zn^{2+}]$ (emission observed at 620 nm).

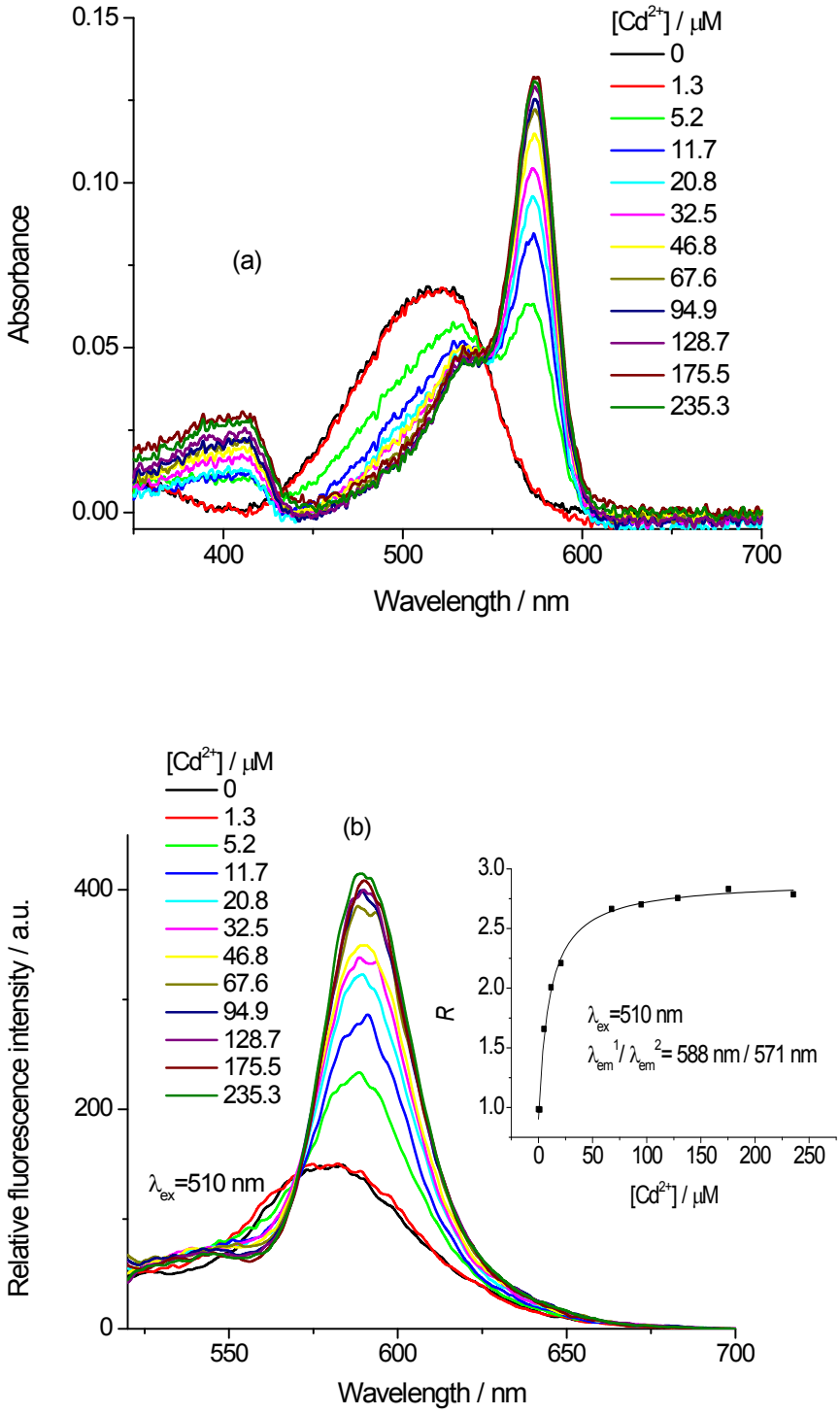

Figure S2. Compound **1** in acetonitrile solution as a function of $[Cd^{2+}]$. (a) Absorption spectra. (b) Fluorescence emission spectra (excitation at 510 nm). The full line in the inset of (b) shows the best fit to the ratiometric emission titration data (eqn 4 with $n = 1$) at $\lambda_{em}^{1}/\lambda_{em}^{2}$ = 588 nm/571 nm (isoemissive point) as a function of $[Cd^{2+}]$.

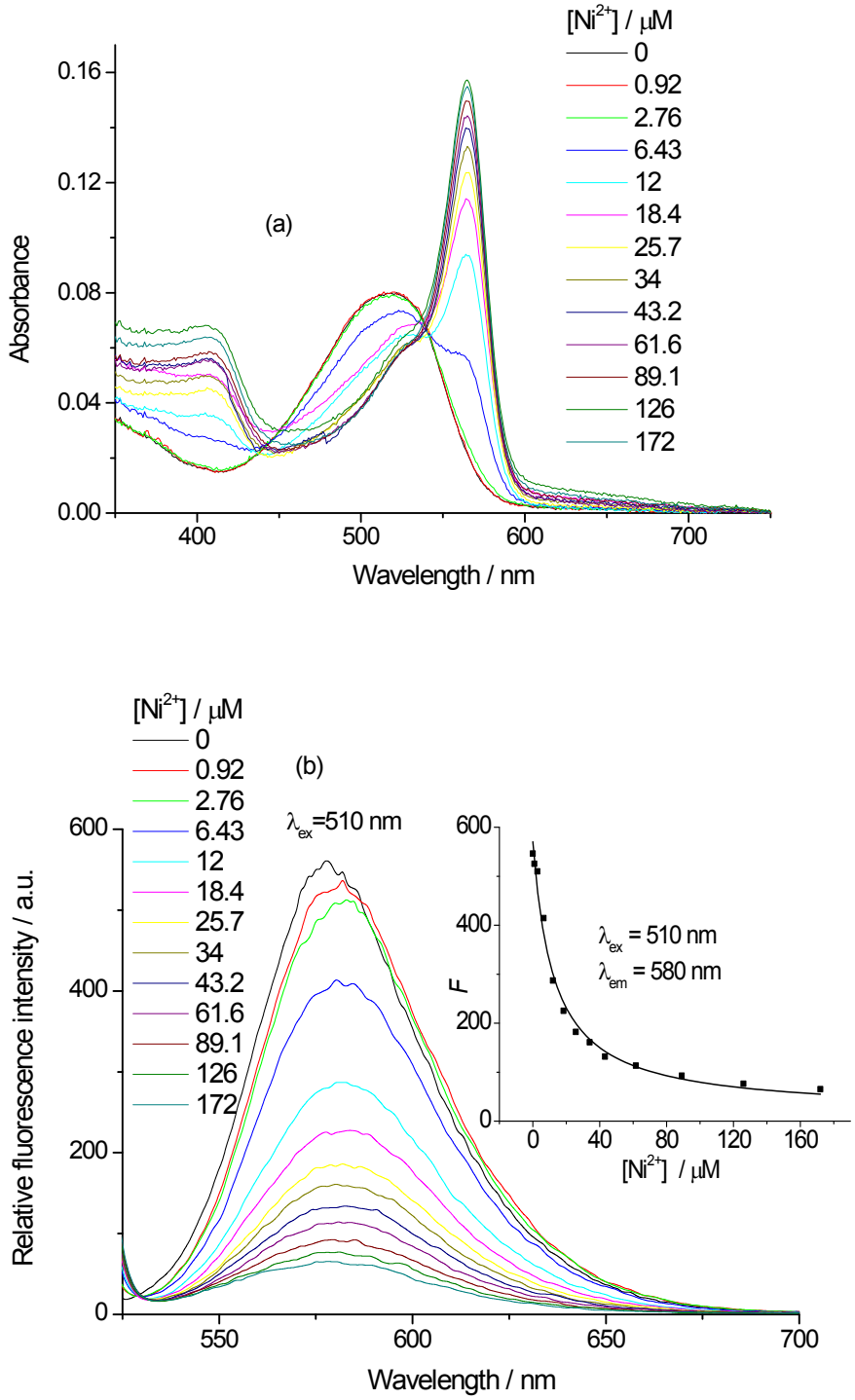

Figure S3. Compound **1** in acetonitrile solution as a function of [Ni^{2+}]. (a) Absorption spectra. (b) Fluorescence emission spectra (excitation at 510 nm). The full line in the inset of (b) shows the best fit to the direct fluorometric emission (eqn 3 with n = 1) titration data at λ_{em} = 580 nm as a function of [Ni^{2+}].

Electrochemistry

Electrochemical data were obtained using a CHI600B potentiostat and a standard three-electrode cell [platinum working and platinum counter electrodes, and a Hg/saturated calomel electrode (SCE) reference] at a scan rate of 100 mV s^{-1}. The voltammograms were recorded at room temperature using a solution of 0.1 mol/L tetrabutylammonium hexafluorophosphate as the supporting electrolyte in dry dichloromethane. All solutions were purged with argon prior to measurement. Figure S4 displays the cyclic voltammogram for **1** showing the one-electron oxidations. The oxidation potentials E_{ox} of **1** estimated from the midpoints of the forward and reverse peaks of the scan appear at ca. +0.82 and +0.97 V vs. SCE, respectively. These values are close to, but somewhat lower than that of the symmetric BODIPY derivative with phenylethynyl groups at the 3,5-positions (E_{ox} = +1.02 V).[4] This indicates that a DPA group is slightly more electron-donating than the phenylethynyl moiety. Substitution of the inductively electron-withdrawing chlorine atom for the DPA subunit in **1** renders oxidation of the chlorine-containing compound more difficult (E_{ox} = +1.52 V).[4] We did not observe any reduction electrochemistry and this may be because these redox potentials are beyond the accessible range of dichloromethane.

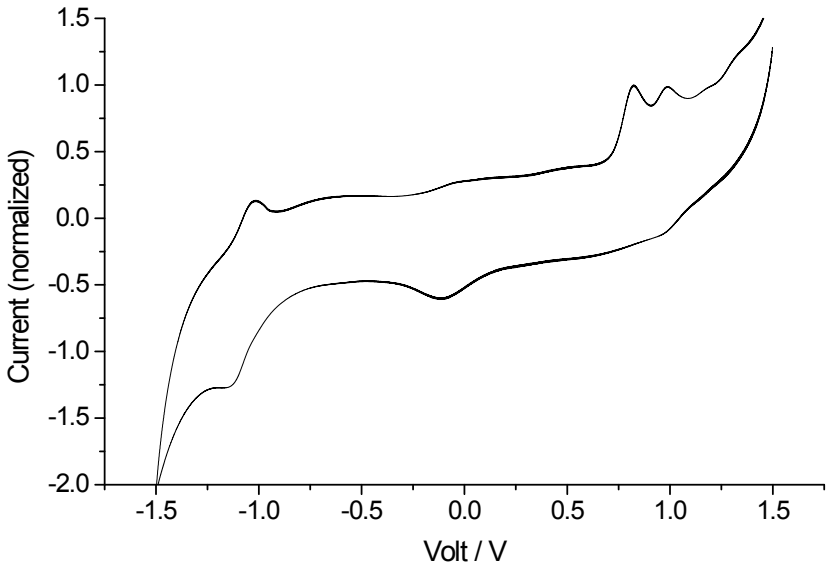

Figure S4. Cyclic voltammogram of **1** in degassed dichloromethane solution containing 0.1 mol L^{-1} tetrabutylammonium hexafluorophosphate using a scan rate of 100 mV s^{-1}. The potentials are expressed vs. a Hg/saturated calomel electrode reference.

Competition experiments

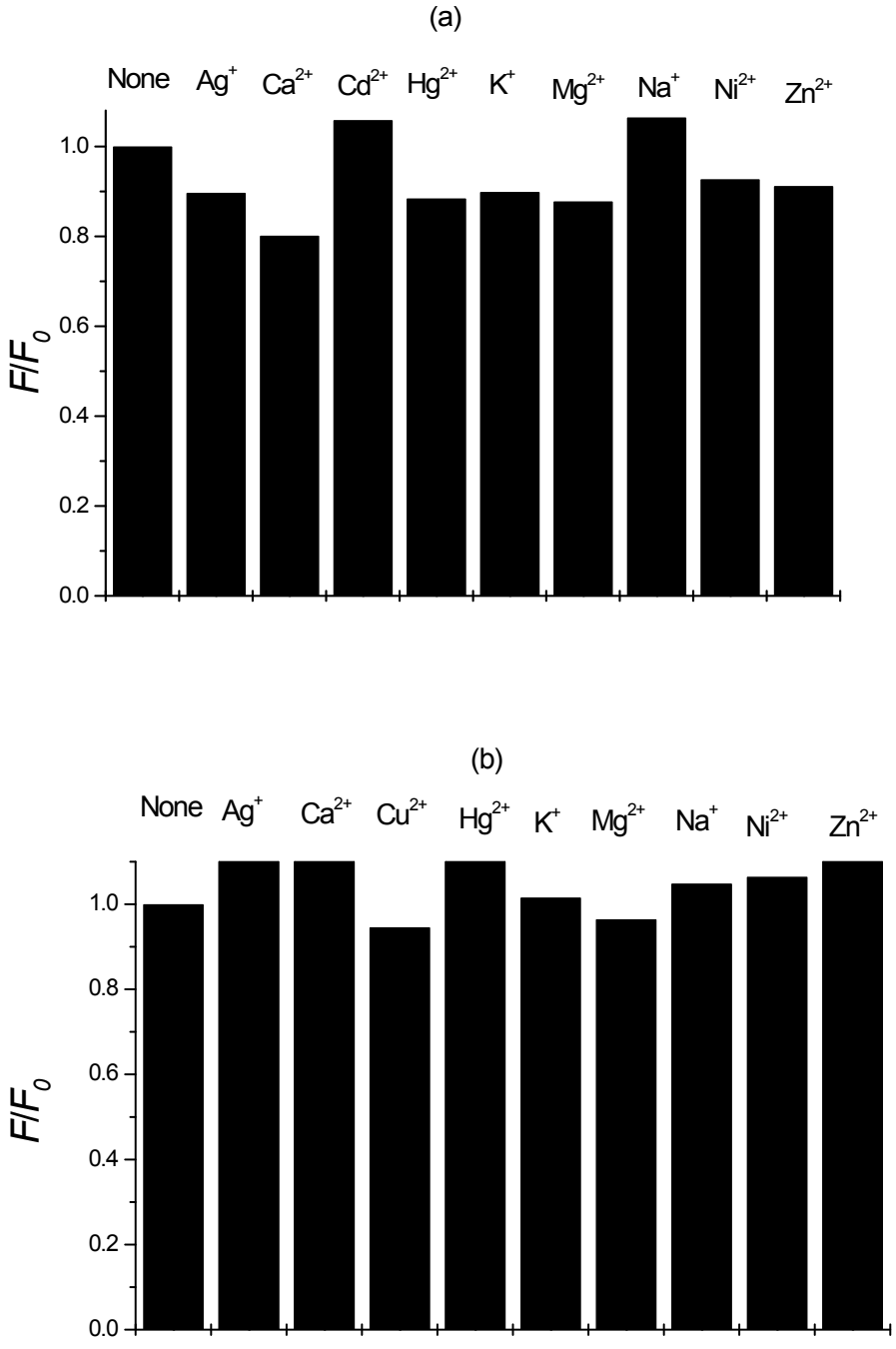

Figure S5. The bars show the fluorescence emission change that occurs to a solution of **1** in the presence of (a) 10 μM Cu^{2+} or (b) 10 μM Cd^{2+} in acetonitrile upon injection of a 50 μM acetonitrile solution of other competing metal ions. The competing ion is indicated on top of each bar. F_0 and F represent the whole, integrated emission spectrum of **1** in the presence of (a) 10 μM Cu^{2+} or (b) 10 μM Cd^{2+}. F_0 is measured in the absence of competing ions, whereas F is obtained in the presence of 50 μM competing ion.

Relationship between *F* and ion concentration

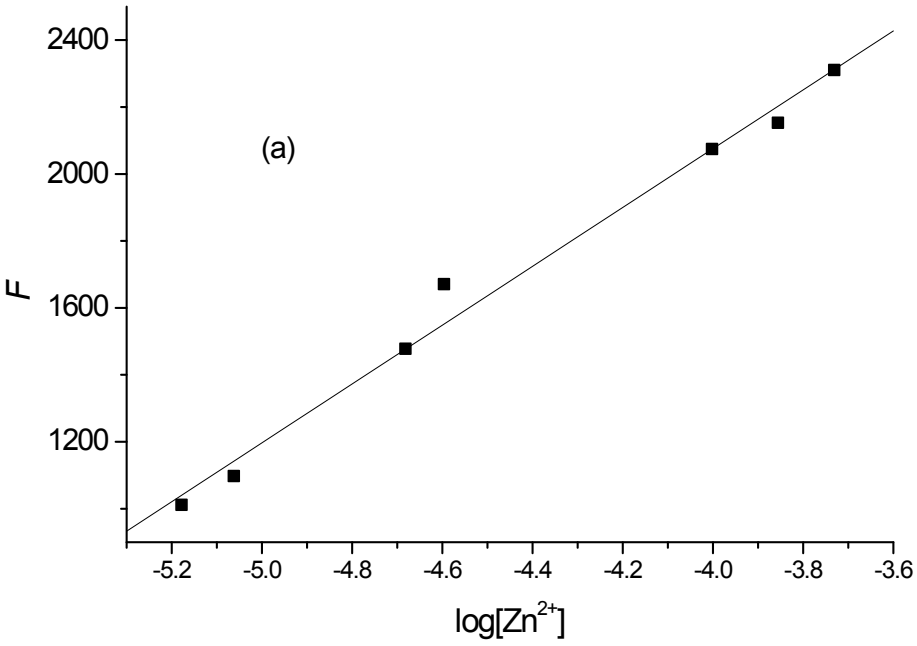

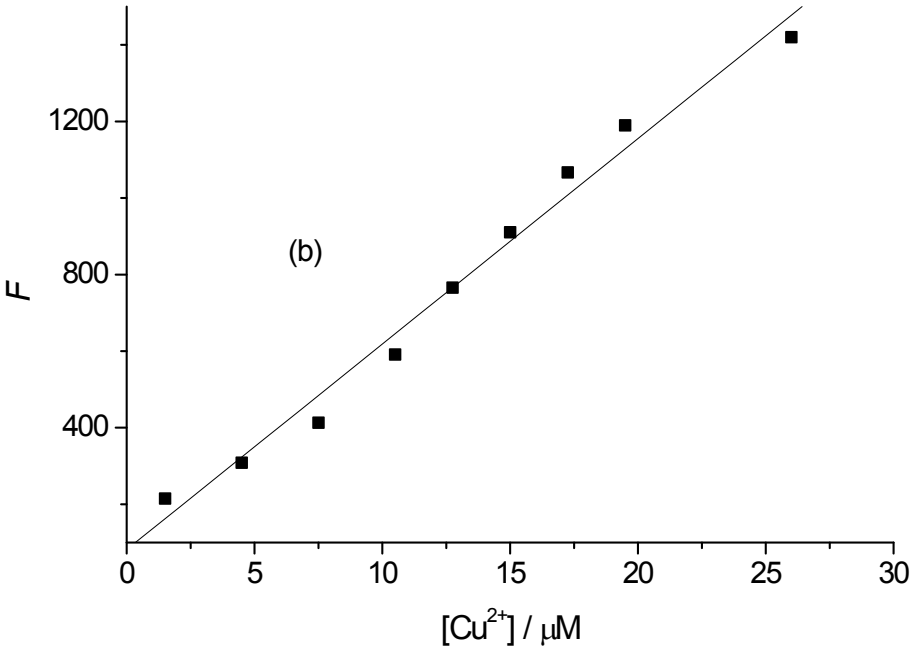

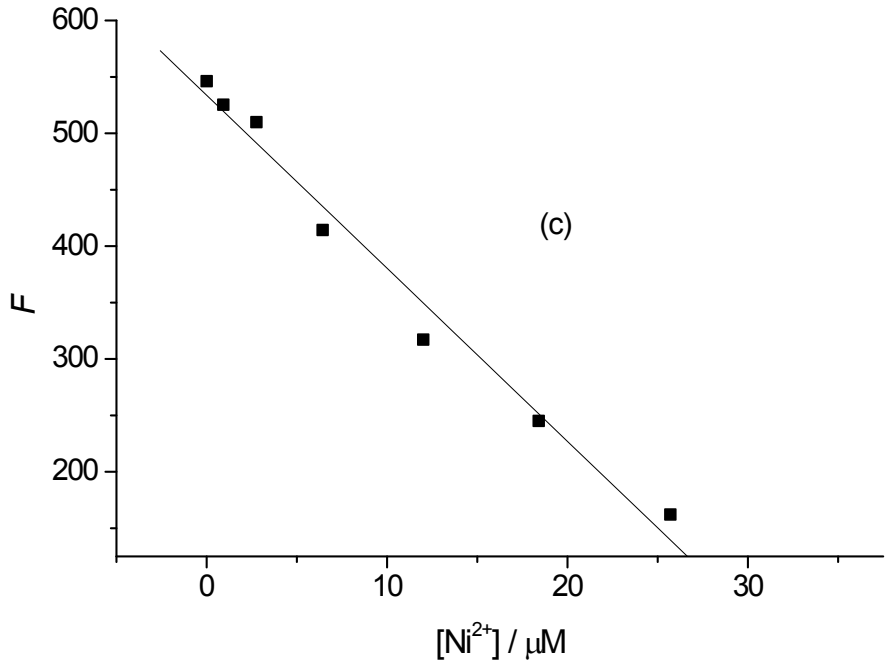

Figure S6. (a) Fluorescence emission *F* measured at 584 nm (λ_{ex} = 510 nm) for **1** in acetonitrile solution as a function of log[Zn^{2+}] ([Zn^{2+}] = 0–280 μM, data obtained from part of the spectra of Figure 3b). (b) Linear relationship between *F* at 616 nm (λ_{ex} = 510 nm) and [Cu^{2+}] ([Cu^{2+}] = 0–25.7 μM, data obtained from part of the spectra of Figure S3b). (c) Linear relationship between *F* at 580 nm (λ_{ex} = 510 nm) and [Ni^{2+}] ([Ni^{2+}] = 0–25.7 μM, data obtained from part of the spectra of Figure 5b).

NMR spectra of 1

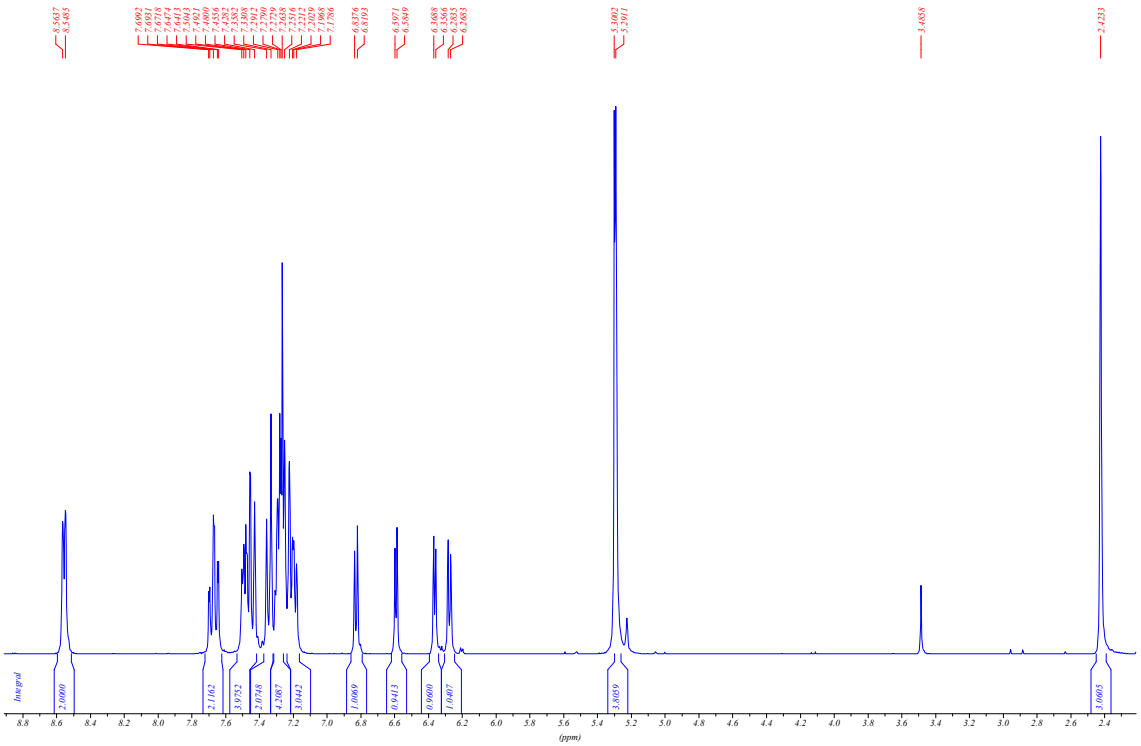

^{1}H NMR of **1** in $CDCl_3$ ↑

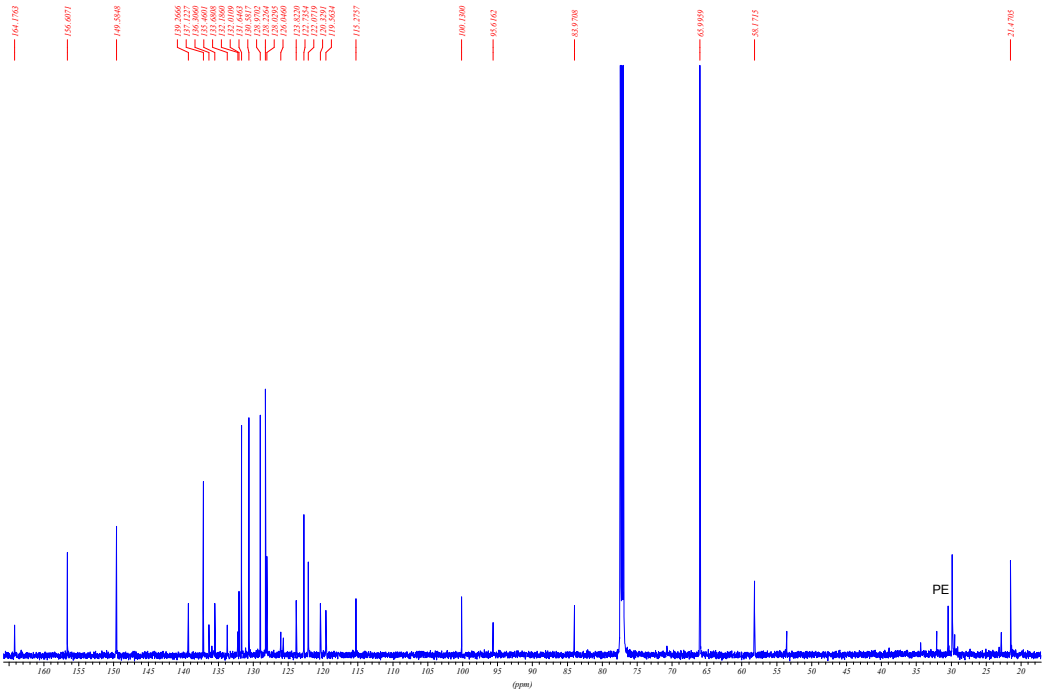

^{13}C NMR of **1** in $CDCl_3$ ↑

References

(1) J. Olmsted, *J. Phys. Chem.*, 1979, **83**, 2581−2584.
(2) E. Cielen, A.. Tahri, A. Ver Heyen, G. J. Hoornaert, F. C. De Schryver and N. Boens, *J. Chem. Soc.*, *Perkin Trans. 2*, 1998, 1573−1580.
(3) J. Catalán, *J. Phys. Chem. B*, 2009, **113**, 5951–5960.
(4) W. Qin, T. Rohand, W. Dehaen, J. N. Clifford, K. Driessen, D. Beljonne, B. Van Averbeke, M. Van der Auweraer and N. Boens, *J. Phys. Chem. A*, 2007, **111**, 8588−8597.